RSC Advances

PAPER

View Article Online
View Journal | View Issue

Cite this: *RSC Adv.*, 2016, **6**, 30160

A selective and economic carbon catalyst from waste for aqueous conversion of fructose into 5-hydroxymethylfurfural†

Tiansheng Deng,‡[a] Jiangong Li,‡[a] Qiqi Yang,[b] Yongxing Yang,[a] Guangqiang Lv,[a] Ying Yao,[c] Limin Qin,[c] Xianlong Zhao,[c] Xiaojing Cui*[a] and Xianglin Hou*[a]

Received 4th January 2016
Accepted 13th March 2016

DOI: 10.1039/c6ra00154h

www.rsc.org/advances

It is of vital importance to design stable and selective heterocatalysts for aqueous production of platforms from biomass-derived sugars. This paper describes a selective aqueous conversion of fructose to HMF using carbon catalysts from pulping waste sodium ligninsulfonate (SLS). The effect of carbonization atmospheres (N_2 flow, static air and air flow) on the structure, porosity, compositions and acidic properties of carbon catalysts were investigated by thermogravimetry-mass spectrum analysis, X-ray photoelectron spectroscopy, Fourier transform infrared spectroscopy, Boehm titrations, N_2 adsorption–desorption isotherms and elemental analysis. The carbonization in air flow favored the formation of more oxygen-containing functional groups and micropores, while more sulfonic groups and meso-/macro-pores were formed during carbonization in a static air atmosphere. Both oxygen- and sulfur-containing groups were acid sites, and their total amount was the largest when carbonized in air flow, followed by static air and N_2 flow. The positive correlation between the acid amounts and fructose conversion of carbon catalysts clearly demonstrated the catalytic effect of the acid sites. The steric hindrance of micropores in carbon catalysts restricted the formation of humins and promoted the HMF selectivity compared with meso-/macro-pores.

Introduction

The increasing shortage of fossil fuels and environmental pollution have stimulated the search for safe and clean energies and chemicals.[1] The potential of biomass as a complement feedstock for fossil resources has been developed because of its abundant and renewable nature.[2] However, biomass resources cannot be utilized directly as fuels due to their low energy density and complex chemical compositions.[3] Increasing efforts have been contributed to convert biomass materials including lignincellulose and saccharides to valuable chemicals,[4] among which the production of 5-hydroxymethylfurfural (HMF) has attracted much attention.[5] HMF is considered as an important platform chemical, which can convert to levulinic acid, dimethylfuran and other biofuels with high heating values.[6]

One of major routes for HMF production is based on acid catalytic dehydration process of fructose.[5,7–23] Organic solvents,[7,9,14,16,22] ionic liquids[10] and biphasic systems (organic/water)[8,11,15] have been demonstrated as the reaction media, and high HMF yields were achieved with the aids of various acid catalysts including heteropoly acids,[21] solid acids,[10,12,20,22] ion exchange resins,[14] zeolites,[15] and acidic ionic liquid.[16] In comparison with organic solvents, water is an environmentally friendly solvent and it is efficient especially for dissolving saccharides. Despite of its green and convenient nature, the studies using water as the reaction medium are few and scarce.[9–11,20] One of the main challenges for using water as solvent is that the high polarity and strong hydrogen bonding interaction of water make many solid acid catalysts unstable, leading to the loss of acid sites in the catalyst. Therefore, homogeneous catalysts are commonly applied in aqueous system. Homogeneous catalysis showed high catalytic efficiency, yet the challenges in the catalyst recycling and separation greatly lower their potential in the commercial application.[12] To tackle these problems, heterogeneous catalysts including mesoporous TiO_2,[9] H_3PO_4 treated Nb_2O_3,[18] aluminosilicate catalysts[15] and heterogeneous zirconium phosphate,[17] were developed to catalyze the conversion of fructose into HMF. Although these catalysts were easily separated, they suffered from low stability. As efficient and stable catalysts, various carbon-based catalysts, such as *p*-styrenesulfonic acid to carbon nanotubes,[13] and graphene oxide[19,24] were developed for fructose dehydration into HMF. However, the expensive carbon material and the complexity in the synthesis of catalyst limit their further application in large-scale industrial production.

[a]*The Biorefinery Research and Engineering Center, Institute of Coal Chemistry, Chinese Academy of Sciences, Taiyuan, 030001, P. R. China. E-mail: cuixj@sxicc.ac.cn; houxl@sxicc.ac.cn*

[b]*Taiyuan University of Technology, Taiyuan, P. R. China*

[c]*Taiyuan Institute of Technology, Taiyuan, P. R. China*

† Electronic supplementary information (ESI) available. See DOI: 10.1039/c6ra00154h

‡ Authors contributed equally.

Another big challenge for HMF synthesis from carbohydrates in water is related to the HMF selectivity. In fact, water promotes the by-products formation, such as levulinic acid, formic acid and polymerized products (humins).[25–27]

Sodium ligninsulfonate (SLS) is popular and could be collected from industrial sewage, such as from pulp liquor.[28] Therefore, SLS derived activated carbon is more economical compared with carbon nanotube and graphene materials. More importantly, we noticed that SLS possesses aromatic structures, and it is rich in sulfonate groups, ether, hydroxyl, and other oxidation groups. The acidic oxygen- and sulfur-containing functional groups, have been demonstrated as the active sites for the dehydration of fructose into HMF.[11–13,24,29] Therefore, the acidic oxygen- and sulfur-containing functional groups in SLS could be preserved after appropriate carbonization process and catalyze the conversion of fructose into HMF. Furthermore, the textural properties of the carbonized catalysts that are crucial to the selective conversion of sugars in water, could be tuned by carbonization conditions.

In the article, SLS was applied as the raw material to fabricate the acidic carbon catalysts for the selective conversion of fructose into HMF in aqueous solution. Three atmospheres were applied for the carbonization of SLS, including N_2 flow, static air atmosphere and air flow. The structure, porosity, compositions and acidic properties of the carbon catalysts after carbonization were investigated by TG-MS, XRD, IR, Boehm titrations, N_2 adsorption–desorption isotherms and elemental analysis, and the fructose conversion and HMF selectivity can be correlated with the acidic properties and porosity of the catalysts, respectively. Yield of 59.9% for HMF can be obtained from fructose in water, and the catalyst were stable after reusing for five times.

Experimental

Materials

Fructose (99%) and 5-hydroxymethylfurfural (HMF) (99%) were obtained from Amresco, J&K Scientific Company and Kermel chemical reagent company (Tianjin, China); sodium ligninsulfonate was purchased from Sigma-Aldrich Corp (USA); phosphoric acid (84 wt%) was from Tianda chemical Corp (Tianjin, China); hydrochloric acid (36 wt%) was obtained from Tianli chemical reagent Co., Ltd. (Tianjin, China); sodium carbonate (99 wt%) was acquired from Beichen Fangzheng chemical reagent Corp (Tianjin, China); sodium hydroxide (96 wt%) was purchased from Henxing chemical reagent Co., Ltd. (Tianjin, China); sodium bicarbonate (99%) was from Beijing Huagong Corp (Beijing, China).

Catalyst preparation and testing

The preparation procedures of phosphoric acid-functionalized carbon catalysts were as follows: 1 g of sodium ligninsulfonate (designated as SLS) was mixed with 2 ml of phosphoric acids, followed by heating in a tube furnace at 500 °C for 2 h statically, or in a nitrogen or air flow with a rate of 80 ml min^{-1}. The heating rate was 18 °C min^{-1}. After being cooled down, the obtained carbon catalysts was mixed with 30 ml hydrochloric acid in a 80 ml Erlenmeyer flask, and the mixture was ultrasonicated for 8 h. The carbon catalysts were then washed by deionized water until a pH of 7 was reached. Finally, the carbon catalysts were dried at 100 °C for 12 h. The phosphoric acid-functionalized carbon catalysts obtained in static air atmosphere, air flow, and N_2 flow were designated as Ct1, Ct2, and Ct3.

The conversion of fructose was performed in a Teflon-lined autoclave with a content of 10 ml. In each test, a certain amount of fructose was dissolved in water, followed by the addition of a certain amount of catalyst. The mixture was maintained at the desired temperature (120–170 °C) and under vigorous stirring. High pressure liquid chromatography (LC-10AT, Shimadzu) was used to analyze the products. The concentration of HMF was analyzed by an UV detector (SPD-10A, Shimadzu) and a 4.6 mm ID250 mm Kromstar C18 reverse-phase column. The mobile phase and the column temperature was acetonitrile solution (70 vol%) with a flow rate of 0.6 ml min^{-1} and 25 °C, respectively. Fructose concentration was obtained by a reflective index detector (RID-10A, Shimadzu) and SC 1011 sugar column (Shodex, Japan). The mobile phase was deionized water with a flow rate of 1 ml min^{-1}, and the column temperature was 80 °C. Standard solutions of HMF and fructose were used to obtain the calibration curves to calculate their concentrations by the external standard method.

Catalyst characterization

Elemental analysis of the samples was carried out using Elementar instrument (Vario Macro Cube, Germany). The powder X-ray diffraction (XRD) patterns were recorded on a X-ray photoelectron spectroscopy (Kratos, UK). Fourier transform infrared spectra of the samples was obtained on a FT-IR analyser (BRUKER TENSOR 27, Germany). The pore structure of the samples were obtained through analyzing N_2 adsorption–desorption isotherms (BEL BELSORP-max, Japan). N_2 adsorption–desorption isotherms was analysed by physical adsorption apparatus (Tristar 3000, USA). The samples were degassed at 100 °C for 8 h prior to the analysis. Thermogravimetric and mass spectrum analysis (TG-MS) was performed on a Evolution 16/18 (Setaram Instrumentation, France) and OMNI star (Pfeiffer Vacuum, Germany). The carrier gas was argon. The temperature was raised from 25 °C to 1000 °C by 10 °C min^{-1}.

Results and discussion

The decomposition behavior of SLS

The mass loss behavior and the phase evolutions of SLS during the carbonization process were investigated by TG-MS. As shown in Fig. 1S and 2S in ESI,† two major stages for the mass loss of SLS were detected by TG, that is, two low-temperature peaks ranging from 150 to 400 °C, and a high-temperature peak ranging from 500 to 900 °C. MS results indicated that carbon oxide (CO), carbon dioxide (CO_2) and methane (CH_4) were generated below 400 °C. Sulfur dioxide (SO_2) was detected when the temperature increased to 230 °C, which can be attributed to the decomposition of sulfonate groups of SLS. The second stage mass loss was accompanied by the generation of

CO and CO_2, which resulted from the further decomposition of the oxidation groups of SLS.

The structure of carbonized catalysts

As indicated by TG-MS results, most of the functional groups of SLS including oxygen- and sulfur-containing groups decomposed in the temperature window of 200–800 °C. It has been demonstrated that these oxygen- and sulfur-containing groups,[11–13,24,29] particularly carboxyl and sulfonic groups[30,31] are catalytic sites for fructose dehydration. Therefore, a carbonization temperature of 500 °C was chosen in order to retain the functional groups in SLS as much as possible and also to carbonize SLS as completely as possible. Moreover, a variety amount of phosphoric acid was added to SLS in the carbonization process to increase the amount of functional groups.[32]

Three atmospheres were chosen for the carbonization of SLS, which include statistic atmosphere, the flow of air and the N_2 flow. The largest mass decline was observed for SLS during carbonization in air flow, whereas the least one was found when SLS was carbonized in N_2 flow (Table 1S, in ESI†). This result indicated more obvious combustion of SLS in air. In addition, the XRD patterns of SLS and the carbonized catalysts are shown in Fig. 3S in ESI.† An obvious peak at 23° and a broad peak at 43° appeared in the carbonized catalysts, which were ascribed to 002 plane and 100 plane of activated carbon structure, respectively.[33] Therefore, the carbonization at 500 °C led to the formation of activated carbon.

The distribution of functional groups in carbonized catalysts

The functional groups in phosphoric acid-functionalized carbon catalysts were investigated by FT-IR (Fig. 4S in ESI†). Vibration at 1715 cm^{-1} can be attributed to carboxyl group ($\nu_{C=O}$), while the band from 1500 cm^{-1} to 1600 cm^{-1} and out of plane bending band at 738 cm^{-1} and 812 cm^{-1} indicate the presence of aromatic structures; the bands of 1360 (δ_{O-H}), 1088 (ν_{C-O}) and 651 cm^{-1} (γ_{O-H}), correspond to hydroxyl of phenol groups, while those for ester bonds (–CO–O–) are at 1280 and 1146 cm^{-1}; the bands of 1210 (ν_{as}) and 1045 cm^{-1} (ν_s) can be attributed to sulfonic groups, while that appearing at 1311 cm^{-1} is the evidence of hydroxyl groups.[34–36]

There existed sulfonic groups, hydroxyl of phenol groups and aromatic structures in the spectrum of SLS. The carbonization in the three atmospheres caused a decline in the band intensities of sulfonic groups and hydroxyl of phenol groups, which is in accordance with the TG-MS results. Meanwhile, the carbonization process led to the formation of carboxyl groups in the three catalysts.

The elemental compositions of SLS and the three phosphoric acid-functionalized carbon catalysts were investigated by ICP-OES. As shown in Table 2S in ESI,† the carbonization process caused the decrease in the contents of oxygen and sulfur in the samples. Combined with FT-IR result, it was concluded that Ct1 catalyst contained more sulfonic groups while Ct2 had more oxygen-containing groups.

To quantify the amount of strong and weak surface acidic sites in the catalysts, Boehm's method was applied.[37,38] In the Boehm's method, the acid sites with weak, moderate or strong acidity can be quantified by acid–base neutralization reaction with strong, moderate or weak base. In our case, $NaHCO_3$ reacts with the strong acid sites including carboxylic and sulfonic groups, Na_2CO_3 is able to neutralize carboxyl, sulfonic and lactone groups, and NaOH can react with all acid sites including carboxyl, sulfonic, lactone and phenolic groups. The amounts of various acid sites calculated by Boehm's method are listed in Table 1.

As shown in Table 1, Ct2 possessed the most acidic sites among the three catalysts, whereas the amount of acidic sites in Ct3 was the least. Noticeably, a positive correlation can be established between the total content of (O + S) (determined by ICP) and the amount of total acid sites for the three catalysts, while such correlation was not found between the oxygen content and the amount of total acid sites for the three catalysts (Fig. 5S and 6S, in ESI†). This result indicated that the acid sites in the catalysts were primarily the oxygen-, and sulfur-containing groups.

The porosity of the carbonized catalysts

As shown in Fig. 7S in ESI,† Ct1 and Ct3 exhibited type II absorption isotherm and Ct2 exhibited type I absorption isotherm. The textural properties and pore size distributions of the three catalysts are shown in Table 2 and Fig. 8S.† Ct2 possessed the highest percentage of micropores, while Ct1 and Ct3 were richer in mesopores and macropores. The carbonization in N_2 flow facilitated the formation of the meso- and macropores, and that in the static air atmosphere favored the formation of both the micro- and mesopores. It is possible that

Table 1 The amounts of acid sites in catalysts determined by Boehm titrations[a]

Catalyst	Carboxyl + sulfonic[b] mmol g^{-1}	Lactone[c] mmol g^{-1}	Phenolic[d] mmol g^{-1}	Total mmol g^{-1}
Ct1	1.2	1.8	5.0	8.0
Ct2	1.7	1.5	10.7	13.9
Ct3	0.6	1.7	4.2	6.5

[a] The acid sites were titrated by $NaHCO_3$ (carboxyl, sulfonic), Na_2CO_3 (carboxyl, sulfonic and lactone) and NaOH (carboxyl, sulfonic, lactone and phenolic), according to ref. 36. [b] Strong acid sites. [c] Moderate acid sites. [d] Weak acid sites.

Table 2 The textural properties of the carbonized catalysts

Catalyst	A_{BET} m^2 g^{-1}	A_{micro}[a] m^2 g^{-1}	V_{total}[b] cm^3 g^{-1}	V_{micro}[a] cm^3 g^{-1}	D[c] nm
Ct1	1054.6	404.3	1.18	0.17	4.5
Ct2	559.4	316.5	0.32	0.13	2.3
Ct3	1198.3	286.3	1.73	0.12	5.8
Ct2[d]	551.8	311.6	0.32	0.13	2.2

[a] The data were from *t*-plot reports. [b] Total pore volume of pores that are less than 323.5 nm diameter. [c] Average pore width. [d] Ct2 after 5-cycled reaction, reaction condition: 170 °C, 0.5 mmol fructose, 5 ml water, 4.5 h.

the majority of meso- and macro-pores in Ct2 were either burned when carbonization in the air flow, as indicated by the great mass loss in this process (Table 1S, in ESI†).

Dehydration of fructose into 5-HMF

The fructose conversions on the three catalysts increased gradually and all reached more than 92% after reaction for 4.5 h (Fig. 9S in ESI†). It has been demonstrated that both the weak and strong acid sites including oxygen- and sulfur-containing functional groups are active towards fructose dehydration.[11–13,24,26–28] The acid amount as a function of the fructose conversion was examined to gain insight into the effect of acid amount on fructose conversion (Fig. 1B). A positive correlation can be established, which clearly demonstrated the catalytic effect of the acid sites on the fructose conversion.

The HMF yield and selectivity of the three catalysts are shown in Fig. 1A and 9S in ESI.† The HMF yield of Ct1 and Ct3 climbed to the maximums at 2.5 and 3 h respectively. In contrast, an increasing enhancement in HMF yield up to 4.5 h was observed on Ct2 (Fig. 1A). After reaction for 4.5 h at 170 °C, HMF selectivity was highest on Ct2, followed by Ct1 and Ct3 (entries 1–3 in Table 3).

As confirmed by BET results (Table 2), the microporous surface area of Ct2 contributed to 56.6% of the total surface area, which was higher than those of Ct1 and Ct3 (38.3% and 23.9% respectively). Moreover, the average pore size of Ct2 was the smallest among all the catalysts. A positive relationship can be established between HMF selectivity and the ratio of microporous to the total surface area, while such correlation was not found between HMF selectivity and the total surface area, or HMF selectivity and the microporous volume (Fig. 1C and 10S in ESI†). These results indicated the promotional effect of the micropores on the HMF selectivity. The promotional effect of micropores on HMF selectivity was also observed in zeolite catalyst systems.[39] The major byproduct was humins in all the test runs in this work. Humins is demonstrated to originate from the polymerization of fructose and HMF.[40–42] By considering the macromolecular nature of humins, it is reasonable to deduce

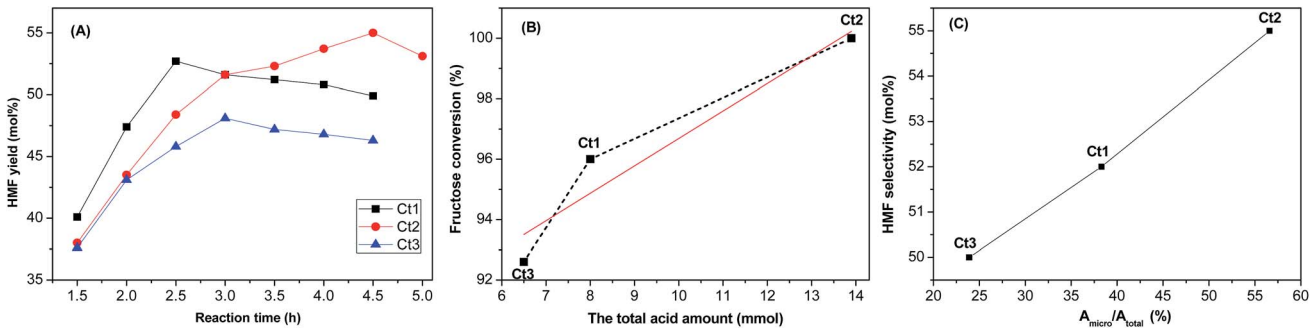

Fig. 1 (A) HMF yield on the three catalysts; correlation of (B) the total acid amount with fructose conversion, and (C) the ratio of the microporous surface area to the total surface area with HMF selectivity.

Table 3 Dehydration of fructose into 5-HMF on the carbonized catalysts[a]

Entry	Catalyst	Temp. °C	Fructose mmol	Cat. loading mg	HMF yield mol%	HMF selectivity mol%	Fructose conv. mol%
1	Ct1	170	1.0	5	49.9	52.0	96.0
2	Ct2	170	1.0	5	55.0	55.0	100.0
3	Ct3	170	1.0	5	46.3	50.0	92.6
4	Ct1	160	1.0	5	41.4	61.3	67.5
5	Ct1	140	1.0	5	7.8	30.8	25.3
6	Ct1	120	1.0	5	0.8	3.3	24.1
7	Ct2	160	1.0	5	50.9	68.3	74.5
8	Ct2	140	1.0	5	7.2	32.5	22.1
9	Ct2	120	1.0	5	0.6	4.1	13.8
10	Ct3	160	1.0	5	36.6	57.8	63.4
11	Ct3	140	1.0	5	6.7	24.1	28.0
12	Ct3	120	1.0	5	0.8	3.0	26.2
13	Ct1	170	0.5	5	50.1	70.7	70.9
14	Ct1	170	2.0	5	48.8	69.4	70.3
15	Ct2	170	0.5	5	55.6	71.1	78.2
16	Ct2	170	2.0	5	59.9	59.9	100.0
17	Ct3	170	0.5	5	46.5	61.6	75.5
18	Ct3	170	2.0	5	40.3	42.7	94.4

[a] Reaction condition: 5 ml of water, 4.5 h.

that the micropores restricted the formation of the humins, and as a result promoted HMF selectivity.

In addition, the effects of reaction conditions including temperature, fructose concentration, and catalyst loading on the HMF yield were investigated. The temperature played an important role in fructose dehydration. Both the fructose conversion were low at the range of 120–140 °C, and they were obviously enhanced at 160–170 °C (Table 3, entries 1–12; Fig. 11S in ESI†). Interestingly, the HMF selectivity of the three catalysts was promoted with increasing temperature. It is likely that at lower reaction temperatures, more fructose molecules were just adsorbed on the catalyst without further conversion. Therefore, the calculated fructose conversion was higher than the real one, causing a lower calculated HMF selectivity.

The effect of catalyst loading and substrate concentration on the fructose dehydration were also investigated (Table 3, entries 1–3, 13–18; Fig. 12S in ESI†). HMF yields of the catalysts were similar with 0.5 or 1.0 mmol fructose in the reaction system. The HMF yield of Ct1 and Ct3 declined with further increase in the amount of fructose to 2.0 mmol. In comparison, the HMF yield of Ct2 increased. In comparison with Ct1 and Ct3, the higher ratio of microporous to the total surface area in Ct2 restricted the formation of the humins, which may account for the enhancement of HMF yield at high fructose concentrations. As shown in Fig. 12S in ESI,† an obvious improvement in the HMF yield occurred when catalyst loading was increased from 3 mg to 5 mg, indicating that HMF formation was promoted with more acid sites. However, the HMF yield declined at high catalyst loadings (20 mg). This result is likely due to the acceleration of side reactions (the formation of humins) at high catalyst loading.

Five-cycled testings were carried out to investigate catalyst stability on fructose dehydration. As shown in Fig. 2, all the three catalysts showed high stability. Particularly, more than 54 mol% of HMF yield can be achieved after the Ct2 catalyst were reused for five times.

Taking into account the sorbent nature of the carbon catalyst, the humins may be adsorbed on the catalyst. By considering the large size of the humins, the adsorbed humins would cause the blockage of micropores and some mesopores in the catalyst, leading to the decrease in the BET surface area and the pore volume of catalysts. The BET analysis of the used catalyst was performed, and the results were listed in the Table 2. Both the BET surface area and the pore volume of the used catalyst were similar to those of the fresh one. This result clearly indicated that the adsorption of humins was trace. These results indicated the great potential of the carbon catalysts Ct2 for the larger-scale selective conversion of fructose in aqueous solution.

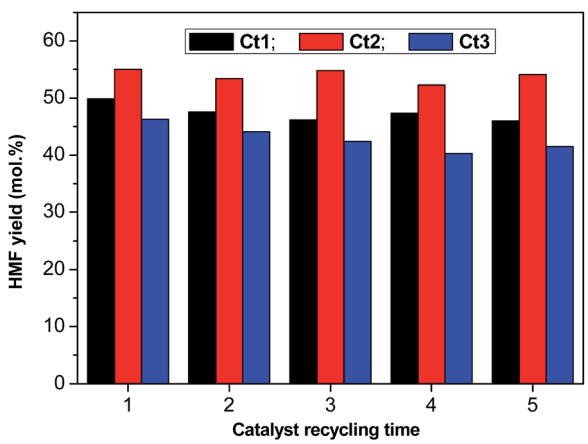

Fig. 2 Five-cycled stability testing on the three catalysts. Reaction condition: 170 °C, 0.5 mmol fructose, 5 ml water, 4.5 h.

Conclusions

We have demonstrated a selective aqueous conversion of fructose into HMF by using carbon catalysts from pulping waste sodium ligninsulfonate. The distribution of functional groups and the porosity of the carbon catalysts were greatly dependent on the carbonization atmosphere. The carbonization in air flow favored the formation of more oxygen-containing functional groups and micropores, while more sulfonic groups and meso-/macro-pores were formed during carbonization in static air atmosphere. These oxygen- and sulfur-containing groups were identified to be the acid sites. The total amount of acid sites increased with the increase in the oxygen concentration in the atmosphere. More meso- and macro-pores were formed during carbonization in the N_2 flow, while micropores were predominant when carbonization in the air flow.

A positive correlation can be established between the acid amounts and the fructose conversions of the carbon catalysts, which clearly demonstrated the catalytic effect of the acid sites. The HMF selectivity was dependent on the porosity of the carbon catalysts. In comparison with the meso- and macropores, the steric hindrance of micropores restricts the formation of humins (the main byproduct), resulting in the promotion in the HMF selectivity. More than 54 mol% of HMF yield (98.4% of the original HMF yield) can be obtained after the catalyst were reused for five times, indicating the promising future of the carbon catalyst for larger-scale production of HMF from fructose.

Acknowledgements

This work was financially supported by the National Key Basic Research Program of China (973 program) (no. 2012CB215305), Science Foundation for Youths of Shanxi (No. 2014021014-5) and the National Natural Science Foundation of China (No. 21303240).

References

1 M. Chatterjee, T. Ishizaka and H. Kawanami, *Green Chem.*, 2014, **16**, 1543.
2 G. W. Huber, S. Iborra and A. Corma, *Chem. Rev.*, 2006, **106**, 4044–4098.
3 Y.-B. Huang and Y. Fu, *Green Chem.*, 2013, **15**, 1095.
4 J. Y. Chan and Y. Zhang, *ChemSusChem*, 2009, **2**, 731–734.
5 H. Zhao, J. E. Holladay, H. Brown and Z. C. Zhang, *Science*, 2007, **316**, 1597–1600.

6 Y. Yang, C.-w. Hu and M. M. Abu-Omar, *Green Chem.*, 2012, **14**, 509–513.
7 J. Wang, T. Qu, M. Liang and Z. Zhao, *RSC Adv.*, 2015, **5**, 106053–106060.
8 S. Wang, H. Lin, J. Chen, Y. Zhao, B. Ru, K. Qiu and J. Zhou, *RSC Adv.*, 2015, **5**, 84014–84021.
9 S. Dutta, S. De, A. K. Patra, M. Sasidharan, A. Bhaumik and B. Saha, *Appl. Catal., A*, 2011, **409–410**, 133–139.
10 L. Hu, G. Zhao, X. Tang, Z. Wu, J. Xu, L. Lin and S. Liu, *Bioresour. Technol.*, 2013, **148**, 501–507.
11 V. V. Ordomsky, J. van der Schaaf, J. C. Schouten and T. A. Nijhuis, *ChemSusChem*, 2012, **5**, 1812–1819.
12 X. Qi, M. Watanabe, T. M. Aida and R. L. Smith Jr, *Catal. Commun.*, 2009, **10**, 1771–1775.
13 R. Liu, J. Chen, X. Huang, L. Chen, L. Ma and X. Li, *Green Chem.*, 2013, **15**, 2895–2903.
14 X. H. Qi, M. Watanabe, T. M. Aida and R. L. Smith, *Ind. Eng. Chem. Res.*, 2008, **47**, 9234–9239.
15 V. V. Ordomsky, J. van der Schaaf, J. C. Schouten and T. A. Nijhuis, *J. Catal.*, 2012, **287**, 68–75.
16 Y. Ma, S. Qing, L. Wang, N. Islam, S. Guan, Z. Gao, X. Mamat, H. Li, W. Eli and T. Wang, *RSC Adv.*, 2015, **5**, 47377–47383.
17 F. S. Asghari and H. Yoshida, *Carbohydr. Res.*, 2006, **341**, 2379–2387.
18 B. Saha and M. M. Abu-Omar, *Green Chem.*, 2014, **16**, 24–38.
19 H. Wang, T. Deng, Y. Wang, X. Cui, Y. Qi, X. Mu, X. Hou and Y. Zhu, *Green Chem.*, 2013, **15**, 2379–2383.
20 A. Dibenedetto, M. Aresta, C. Pastore, L. di Bitonto, A. Angelini and E. Quaranta, *RSC Adv.*, 2015, **5**, 26941–26948.
21 Q. Zhao, Z. Sun, S. Wang, G. Huang, X. Wang and Z. Jiang, *RSC Adv.*, 2014, **4**, 63055–63061.
22 N. Wang, Y. Yao, W. Li, Y. Yang, Z. Song, W. Liu, H. Wang, X.-F. Xia and H. Gao, *RSC Adv.*, 2014, **4**, 57164–57172.
23 A. A. Assanosi, M. M. Farah, J. Wood and B. Al-Duri, *RSC Adv.*, 2014, **4**, 39359–39364.
24 H. Wang, Q. Kong, Y. Wang, T. Deng, C. Chen, X. Hou and Y. Zhu, *ChemCatChem*, 2014, **6**, 728–732.
25 W. Xing, H. H. Ngo, S. H. Kim, W. S. Guo and P. Hagare, *Bioresour. Technol.*, 2008, **99**, 8674–8678.
26 T. S. Deng, X. J. Cui, Y. Q. Qi, Y. X. Wang, X. L. Hou and Y. L. Zhu, *Chem. Commun.*, 2012, **48**, 5494–5496.
27 J. S. Kruger, V. Nikolakis and D. G. Vlachos, *Appl. Catal., A*, 2014, **469**, 116–123.
28 Y. Román-Leshkov, J. N. Chheda and J. A. Dumesic, *Science*, 2006, **312**, 1933–1937.
29 X. Zhang, M. Wang, Y. Wang, C. Zhang, Z. Zhang, F. Wang and J. Xu, *Chin. J. Catal.*, 2014, **35**, 703–708.
30 B. R. Caes, M. J. Palte and R. T. Raines, *Chem. Sci.*, 2013, **4**, 196–199.
31 S. Kang, J. Ye, Y. Zhang and J. Chang, *RSC Adv.*, 2013, **3**, 7360.
32 Y. Chen, S.-R. Zhai, N. Liu, Y. Song, Q.-D. An and X.-W. Song, *Bioresour. Technol.*, 2013, **144**, 401–409.
33 T. Tsoncheva, I. Genova, B. Tsintsarski, M. Dimitrov, D. Paneva, Z. Zheleva, I. Yordanova, G. Issa, D. Kovacheva, T. Budinova, H. Kolev, R. Ivanova, I. Mitov and N. Petrov, *React. Kinet., Mech. Catal.*, 2013, **110**, 281–294.
34 J. M. V. Nabais, C. Laginhas, P. J. M. Carrott and M. M. L. R. Carrott, *J. Anal. Appl. Pyrolysis*, 2010, **87**, 8–13.
35 J. M. V. Nabais, P. Nunes, P. J. M. Carrott, M. M. L. Ribeiro Carrott, A. M. García and M. A. Díaz-Díez, *Fuel Process. Technol.*, 2008, **89**, 262–268.
36 J. M. V. Nabais, C. E. C. Laginhas, P. J. M. Carrott and M. M. L. Ribeiro Carrott, *Fuel Process. Technol.*, 2011, **92**, 234–240.
37 H. P. Boehm, E. Diehl, W. Heck and R. Sappok, *Angew. Chem., Int. Ed. Engl.*, 1964, **3**, 669–677.
38 Z. J. Jiang, Y. Liu, X. P. Sun, F. P. Tian, F. X. Sun, C. H. Liang, W. S. You, C. R. Han and C. Li, *Langmuir*, 2003, **19**, 731–736.
39 C. Moreau, R. Durand, S. Razigade, J. Duhamet, P. Faugeras, *et al.*, *Appl. Catal., A*, 1996, **145**, 211–224.
40 K. Shimizu, R. Uozumi and A. Satsuma, *Catal. Commun.*, 2009, **10**, 1849–1853.
41 C. H. Kuo, A. S. Poyraz, L. Jin, Y. T. Meng, L. Pahalagedara, S. Y. Chen, D. A. Kriz, C. Guild, A. Gudza and S. L. Suib, *Green Chem.*, 2014, **16**, 785–791.
42 L. Wang, H. Wang, F. J. Liu, A. M. Zheng, J. Zhang, Q. Sun, J. P. Lewis, L. F. Zhu, X. J. Meng and F. S. Xiao, *ChemSusChem*, 2014, **7**, 402–406.